

# Journal of **Pharmacology and Toxicology**

ISSN 1816-496X



# Molecular Modelling Analysis of the Metabolism of Thiabendazole

# Fazlul Huq

Discipline of Biomedical Science, School of Medical Sciences, Faculty of Medicine, Cumberland Campus, C42, the University of Sydney, Lidcombe, Nsw, Australia

**Abstract:** Thiabendazole (TBZ) is a broad-spectrum anthelmintic that is effective against gastrointestinal nematodes in ruminants and lungworms in sheep. Molecular modelling analyses based on molecular mechanics, semi-empirical (PM3) and DFT (at B3LYP/6-31G\* level) calculations show that TBZ and its metabolites have moderately large LUMO-HOMO energy differences except 5K-TBZ which has a much smaller value. The results indicate that generally TBZ and its metabolites would be fairly inert kinetically except 5K-TBZ which would be highly labile. The molecular surfaces of TBZ and its metabolites are found to possess neutral (green) and negative (yellow and red) and some electron-deficient (blue) regions so that they may be subject to lyophilic, electrophilic and nucleophilic interactions. Terminal metabolite TBZ-5S is found to abound most in electron-rich negative regions so that it may be most subject to electrophilic attack whereas the most reactive metabolite 5K-TBZ is found to abound most in electron-deficient regions so that it can be most subject to nucleophilic attack. Nucleophilic attack to the electron-deficient sites may be due to glutathione and nucleobases in DNA resulting into glutathione depletion and oxidation of nucleobases. Depletion of glutathione depletion would induce oxidative stress and hence cellular toxicity whereas oxidation of nucleobases in DNA would cause DNA damage.

**Key words:** Thiabendazole, anthelmintic, nematodes, lungworms, fungicide, molecular modelling

# INTRODUCTION

Thiabendazole (TBZ; 2-(4-thiazolyl)-1*H*-benzimidazole) is a broad-spectrum anthelmintic that is effective against parasitic infections in domestic animals and humans e.g., gastrointestinal nematodes in ruminants and lungworms in sheep (McKellar and Scott, 1990; Dalvie *et al.*, 2006). TBZ is also a versatile fungicide that is widely used both pre- and post-harvest to control a range of pathogenic fungi affecting field crops and stored fruits (e.g., banana and citrus fruits) and vegetables (Cannavan *et al.*, 1998). Since its introduction about 40 years ago, although other benzimadzole with improved efficacy, such as albendazole, have been developed, TBZ remains in use because of low cost. After oral administration to farm animals and human, TBZ is absorbed rapidly from the gastrointestinal tract and excreted via urine and faeces (Chukwudebe *et al.*, 1994).

The use of TBZ as a fungicide provides a possible route for entry of its residues into the human food chain, either through direct exposure or through exposure of food-producing animals such as chickens and cattle to feed from TBZ-treated plants (VandenHeuvel *et al.*, 1996). TBZ was found to cause severe kidney toxicity in male mice depleted of glutathione (GSH) by pre-treatment with Buthionine Sulf Oxamine (BSO) which is an inhibitor of GSH synthesis (Mizutani *et al.*, 1990). The injury is characterized by increases in kidney weight and concentration of Serum Urea Nitrogen (SUN) and tubular necrosis (Mizutani *et al.*, 1993).

The drug is extensively metabolized in farm animals and humans via hydroxylation of the benzimidazole ring at the 5-position to form the major metabolite 5-hydroxythiabendazole (5HTBZ)

Fig. 1: Metabolic pathways for TBZ adapted from Chukwudebe et al. (1994)

which is then conjugated with glucuronic acid and sulfate to form corresponding glucuronide (TBZ-5-GLUand sulfate (TBZ-5S) respectively (Chukwudebe *et al.*, 1994). It has been proposed that metabolic activation of 5HTBZ involves its oxidation to quinone imine (5KTBZ) (Dalvie *et al.*, 2006). 5HTBZ can be further hydroxylated to produce such metabolites as 5,6-dihydroxythiabendazole (5,6-DHTBZ). A minor metabolite of TBZ is 4-Hydroxythiabendazole (4HTBZ) formed by hydroxylation of the benzimidazole ring at the 4-position. Another metabolite produced is BenzimidaZole (BZ). In rodents, N-methylthiabendazole and 2-acetylbenzimidazole have also been identified as minor urinary metabolites (Tsuchiya *et al.*, 1987; Fujitani *et al.*, 1991).

In this study, molecular modelling analyses have been carried out using the program Spartan '02 (2002) to investigate the relative stability of TBZ and its metabolites 4HTBZ, 5HTBZ, BZ, TBZ-5S, TBZ-5-GLU, 5K-TBZ and 5,6-DHTBZ with the aim of providing a better understanding on their relative toxicity. The study was carried out in the Discipline of Biomedical Science, School of Medical Sciences, The University of Sydney during the months of December 2006 to January 2007.

# COMPUTATIONAL METHODS

The geometries of TBZ and its metabolites (Fig. 1) 4HTBZ, 5HTBZ, BZ, TBZ-5-S, TBZ-5-GLU, 5K-TBZ and 5,6-DHTBZ have been optimised based on molecular mechanics, semi-empirical and DFT calculations, using the molecular modelling program Spartan '02 (2002). Molecular mechanics calculations were carried out using MMFF force field. Semi-empirical calculations were carried out using the routine PM3. DFT (Density Functional Theory) calculations were carried at B3LYP/6-31G\* level. In optimization calculations, a RMS gradient of 0.001 was set as the terminating condition. For

the optimised structures, single point calculations were carried out to give heat of formation, enthalpy, entropy, free energy, dipole moment, solvation energy, energies for HOMO (highest occupied molecular orbital) and LUMO (lowest unoccupied molecular orbital). The order of calculations: molecular mechanics followed by semi-empirical followed by DFT ensured that the structure was not embedded in a local minimum. To further check whether the global minimum was reached, some calculations were carried out with improvable structures. It was found that when the stated order was followed, structure corresponding to the global minimum or close to that could ultimately be reached in all cases. Although RMS gradient of 0.001 may not be sufficiently low for vibrational analysis, it is believed to be sufficient for calculations associated with electronic energy levels.

# RESULTS AND DISCUSSION

Table 1 gives the total energy, heat of formation as per PM3 calculation, enthalpy, entropy, free energy, surface area, volume, dipole moment and energies of HOMO and LUMO as per both PM3 and DFT calculations for TBZ and its metabolites 4HTBZ, 5HTBZ, BZ, TBZ-5S, TBZ-5-GLU, 5K-TBZ and 5,6-DHTBZ. Figure 2-9 give the regions of negative electrostatic potential (greyish-white envelopes) in (a), HOMOs (where red indicates HOMOs with high electron density) in (b), LUMOs in © and density of electrostatic potential on the molecular surface (where red indicates negative, blue indicates positive and green indicates neutral) in (d) as applied to the optimised structures of TBZ and its metabolites 4HTBZ, 5HTBZ, BZ, TBZ-5S, TBZ-5-GLU, 5KDBZ and 5,6-DHTBZ.

Molecule	Calculation type	Total energy (kcal mol <sup>-1</sup> / atomic unit*)	Heat of formation (kcal mol <sup>-1</sup> )	Enthalpy (kcal mol <sup>-1</sup> )	Entropy (kcal mol <sup>-1</sup> K <sup>-1</sup> )	Free energy (kcal mol <sup>-1</sup> )	Solvation energy (cal mol <sup>-1</sup> K <sup>-1</sup> )
TBZ	PM3	74.56	90.91	101.52	102.80	70.87	-16.34
411770.77	DFT	-947.72	44.25	102.38	97.24	73.39	-16.49
4HTBZ	PM3	27.26	44.25	106.48	109.07	73.96	-16.99
	DFT	-1022.94		106.58	107.77	74.45	-16.04
5HTBZ	PM3	27.60	48.31	104.90	106.89	73.03	-20.70
7.7	DFT	-1022.94	.=	106.12	108.72	73.71	-23.06
BZ	PM3	35.29	47.76	76.88	80.62	52.85	-12.46
	DFT	-379.89		78.19	78.28	54.85	-13.19
TBZ-5S	PM3	-110.05	-81.61	116.48	135.14	76.18	-28.44
	DFT	-1646.74		118.21	134.08	78.25	-29.69
TBZ-5-GLU		-283.68	-247.72	213.22	173.41	161.51	-35.96
	DFT	-1782.94		215.68	172.07	164.40	-36.20
5K-TBZ	PM3	77.28	89.82	99.10	107.70	66.99	-12.54
	DFT	-1005.63		97.47	102.44	66.93	-11.54
5,6-DHTBZ		-22.17	-1.89	110.45	116.22	75.80	-20.28
	DFT	-1098.16		112.23	115.08	77.94	-21.67
	Calculation	Area	Volume	Dipole moment		LUMO	LUMO-HOMO
Molecule	type	(Å2)	(Å3)	(debye)	(eV)	(eV)	(eV)
TBZ	PM3	209.40	191.60	4.0	-8.86	-1.08	7.78
	DFT	207.72	190.42	4.3	-5.81	-1.36	4.45
4HTBZ	PM3	218.85	198.76	4.2	-8.60	-1.07	7.53
	DFT	216.09	197.40	4.9	-5.50	-1.40	4.10
5HTBZ	PM3	218.68	198.85	4.8	-8.93	-1.13	7.80
	DFT	216.76	197.59	5.3	-5.52	-1.34	4.18
BZ	PM3	142.51	126.23	3.3	-8.89	-0.09	8.80
	DFT	141.53	125.38	3.4	-6.07	-0.34	5.73
TBZ-5S	PM3	271.66	240.72	5.5	-9.04	-1.16	7.88
	DFT	267.11	239.04	8.1	-6.24	-1.69	4.55
TBZ-5-GLU		372.87	346.58	6.3	-9.11	-1.14	7.97
	DFT	364.34	343.27	3.9	-5.65	-1.30	4.35
5K-TBZ	PM3	216.85	200.80	2.4	-9.29	-2.19	7.10
	DFT	216.05	200.07	3.3	-6.03	-3.62	2.41
5,6-DHTBZ		226.95	205.87	4.2	-8.57	-0.98	7.59
	DFT	224.26	204.35	4.7	-5.18	-1.20	3.98

<sup>\*</sup>In atomic units from DFT calculations

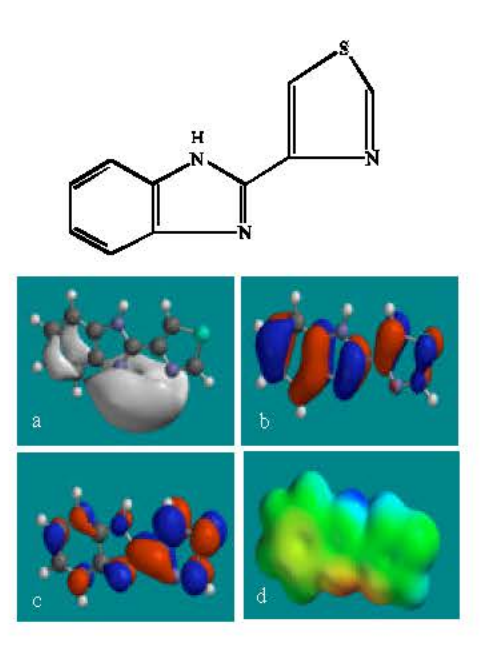


Fig. 2: Structure of TBZ giving in: (a) the electrostatic potential (greyish envelope denotes negative electrostatic potential), (b) the HOMOs, (where red indicates HOMOs with high electron density) (c) the LUMOs (where blue indicates LUMOs) and in (d) density of electrostatic potential on the molecular surface (where red indicates negative, blue indicates positive and green indicates neutral)

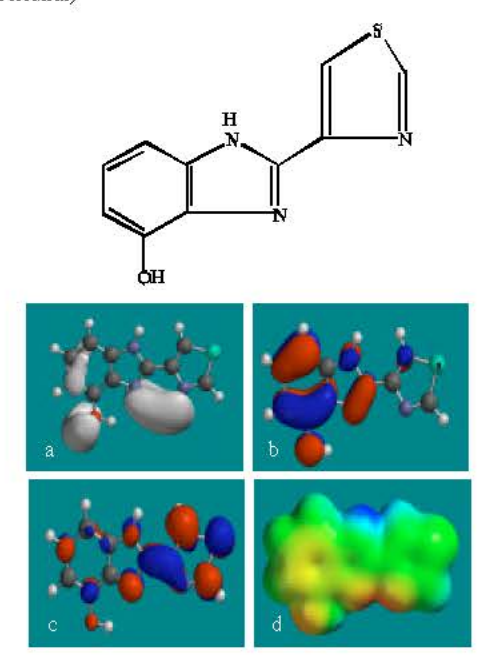


Fig. 3: Structure of 4HTBZ giving in: (a) the electrostatic potential greyish envelope denotes negative electrostatic potential), (b) the HOMOs, (where red indicates HOMOs with high electron density) (c) the LUMOs (where blue indicates LUMOs) and in (d) density of electrostatic potential on the molecular surface (where red indicates negative, blue indicates positive and green indicates neutral)

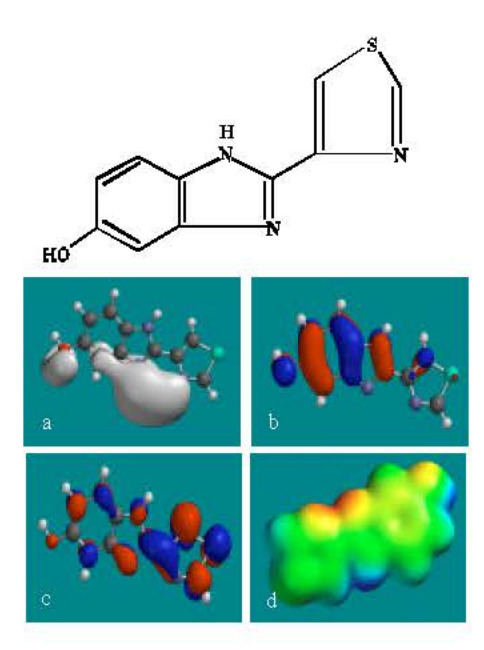


Fig. 4: Structure of 5HTBZ giving in: (a) the electrostatic potential greyish envelope denotes negative electrostatic potential), (b) the HOMOs, (where red indicates HOMOs with high electron density) (c) the LUMOs (where blue indicates LUMOs) and in (d) density of electrostatic potential on the molecular surface (where red indicates negative, blue indicates positive and green indicates neutral)

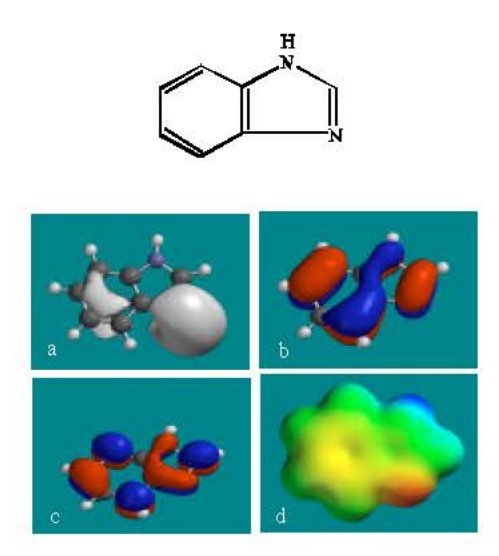


Fig. 5: Structure of BZ giving in: (a) the electrostatic potential (greyish envelope denotes negative electrostatic potential), (b) the HOMOs, (where red indicates HOMOs with high electron density) (c) the LUMOs (where blue indicates LUMOs) and in (d) density of electrostatic potential on the molecular surface (where red indicates negative, blue indicates positive and green indicates neutral)

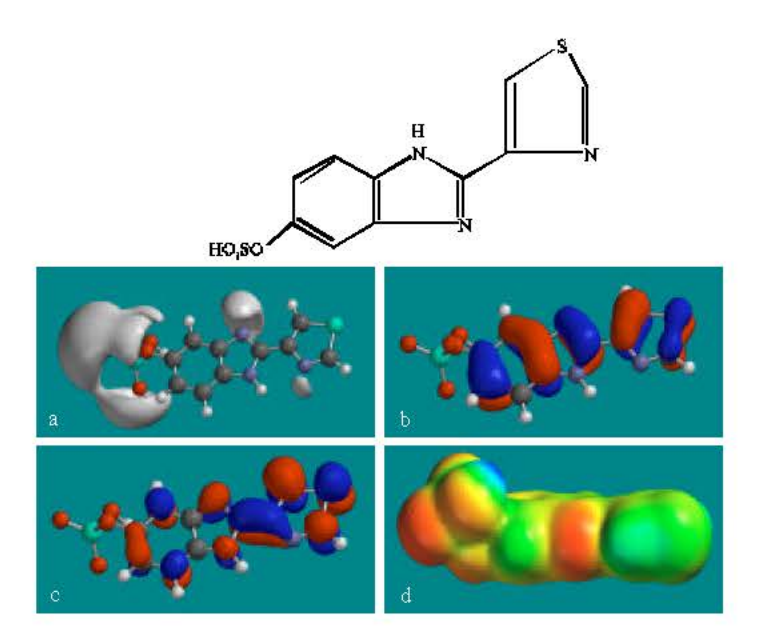


Fig. 6: Structure of TBZ-5S giving in: (a) the electrostatic potential (greyish envelope denotes negative electrostatic potential), (b) the HOMOs, (where red indicates HOMOs with high electron density) (c) the LUMOs (where blue indicates LUMOs) and in (d) density of electrostatic potential on the molecular surface (where red indicates negative, blue indicates positive and green indicates neutral)

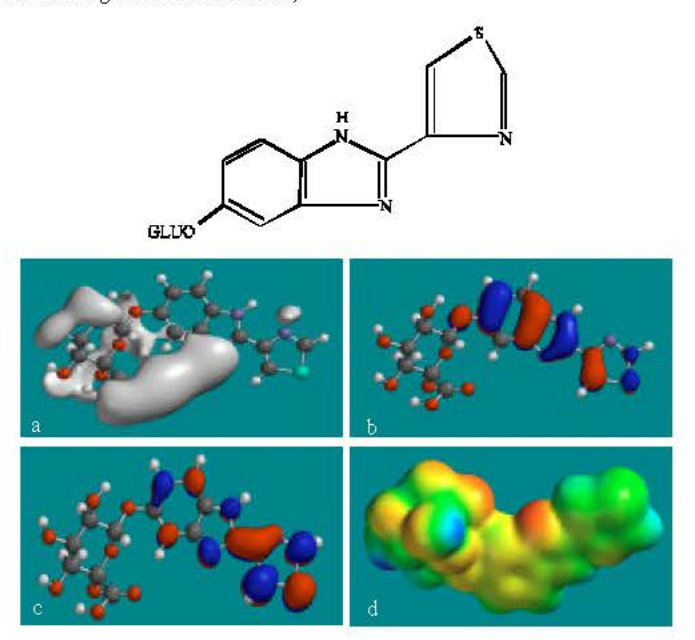


Fig. 7: Structure of TBZ-5-GLU giving in: (a) the electrostatic potential (greyish envelope denotes negative electrostatic potential), (b) the HOMOs, (where red indicates HOMOs with high electron density) (c) the LUMOs (where blue indicates LUMOs) and in (d) density of electrostatic potential on the molecular surface (where red indicates negative, blue indicates positive and green indicates neutral)

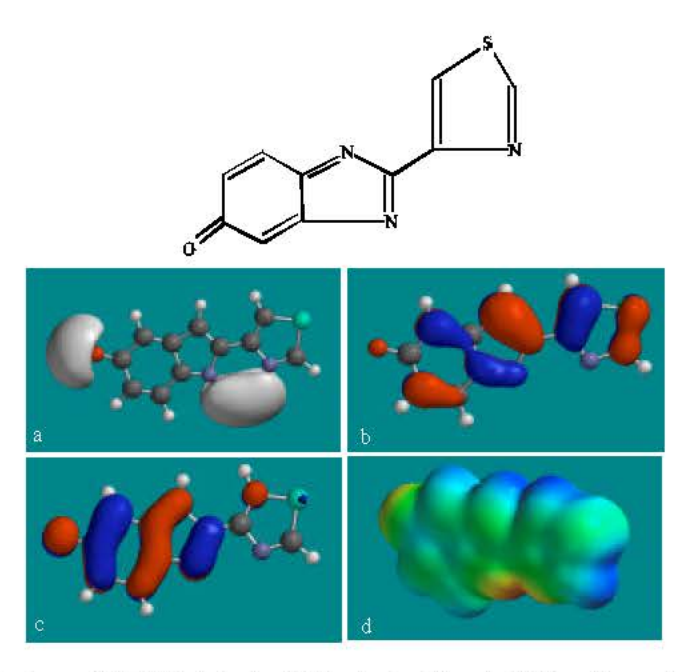


Fig. 8: Structure of 5K-TBZ giving in: (a) the electrostatic potential (greyish envelope denotes negative electrostatic potential), (b) the HOMOs, (where red indicates HOMOs with high electron density) (c) the LUMOs (where blue indicates LUMOs) and in (d) density of electrostatic potential on the molecular surface (where red indicates negative, blue indicates positive and green indicates neutral)

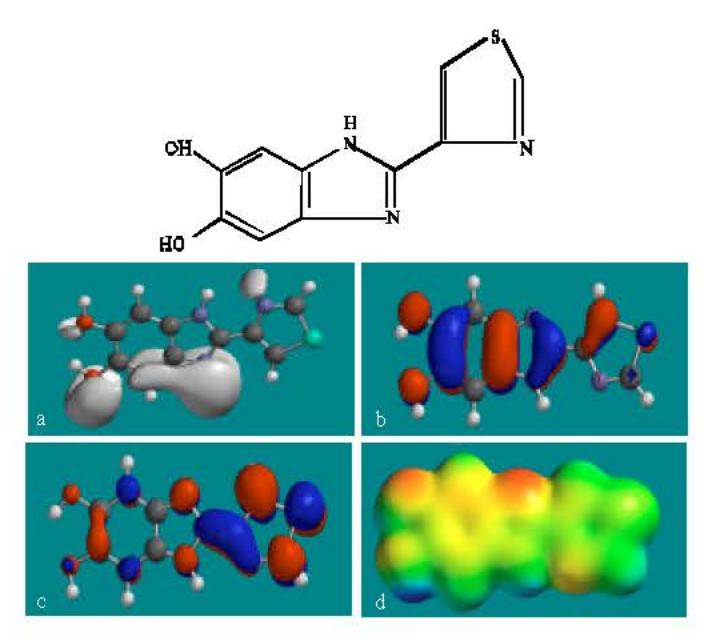


Fig 9: Structure of 5,6-DHTBZ giving in: (a) the electrostatic potential (greyish envelope denotes negative electrostatic potential), (b) the HOMOs, (where red indicates HOMOs with high electron density) (c) the LUMOs (where blue indicates LUMOs) and in (d) density of electrostatic potential on the molecular surface (where red indicates negative, blue indicates positive and green indicates neutral)

The calculated solvation energies from PM3 calculations of TBZ and its metabolites 4HTBZ, 5HTBZ, BZ, TBZ-5-S, TBZ-5-GLU, 5KDBZ and 5,6-DHTBZ are respectively -16.34, -16.99, -20.70, -12.46, -28.44, -35.96, -12.54 and -20.28 and corresponding dipole moments from DFT calculations are 4.3, 4.9, 5.3, 3.4, 8.1, 3.9, 3.3 and 4.7. The values suggest that among TBZ and its metabolites 5k-TBZ and BZ would have the lowest solubility in water and terminal metabolites TBZ-5-GLU and TBZ-5S would have much higher solubility.

The LUMO-HOMO energy differences for TBZ and its metabolites from DFT calculations are found to be high ranging from 2.4 to 5.7 eV indicating that TBZ and its metabolites would vary in their kinetic lability with 5K-TBZ being most labile and BZ being most inert.

In the case of TBZ, the electrostatic potential is found to be more negative around the various nitrogen centres and above and below the phenyl ring, indicating that the positions may be subject to electrophilic attack. In the case of 5H-TBZ, 4H-TBZ, TBZ-5S and TBZ-5-GLU, the electrostatic potential is found to be negative around nitrogen and oxygen centres, indicating that the positions may be subject to electrophilic attack. In the case of BZ, the electrostatic potential is found to be negative around nitrogen centres and above and below the phenyl ring, indicating that the positions may be subject to electrophilic attack.

In the case of TBZ, 4HTBZ, 5HTBZ, TBZ-5K and 5,6-DKTBZ, both the HOMOs with high electron density and the LUMOs are found to be centred on most of the non-hydrogen atoms. In the case of TBZ-5S also, both the HOMOs with high electron density and the LUMOs are found to be centred on most of the non-hydrogen atoms except those of the sulfate In the case of TBZ-5-GLU, both the HOMOs with high electron density and the LUMOs are found to be centred on most of the non-hydrogen atoms except those of the glucorunic acid moiety.

The overlap of HOMO with high electron density and region of negative electrostatic potential at some positions, gives further support to the idea that the positions may be subject to electrophilic attack.

The molecular surfaces of TBZ, 4HTBZ, 5HTBZ and BZ, are found to abound in neutral (green) regions and in addition possess some electron-rich and electron-deficient regions so that they may be subject to lyophilic, electrophilic and nucleophilic attacks. The molecular surfaces of TBZ-5S, TBZ-5-GLU and 5,6-DKTBZ, are found to abound in electron-rich regions so that they may be more likely subject to electrophilic attacks. The molecular surface of TBZ-5K is found to abound most in electron-deficient regions so that it may be most subject to nucleophilic attacks such as those by glutathione and nucleobases in DNA. Reaction with glutathione will induce cellular toxicity by compromising the antioxidant status of the cell whereas that with nucleobases in DNA will cause DNA damage. As stated earlier, since TBZ-5K is expected to be highly labile, the effects of such adverse reactions is expected to be quite significant so that toxicity of TBZ may be due to TBZ-5K.

# CONCLUSION

Thiabendazole is a broad-spectrum anthelmintic that is effective against gastrointestinal nematodes in ruminants and lungworms in sheep Molecular modelling analyses based on semi-empirical and DFT calculations show that TBZ and its metabolites have large LUMO-HOMO energy differences except TBZ-5K which has a much smaller value. This means that TBZ-5K would be labile kinetically whereas TBZ and rest of the metabolites would be kinetically inert. The high lability of TBZ-5K and the abundance of electron-deficient regions on its molecular surface means that the metabolite can react readily with glutathione and nucleobases in DNA, causing glutathione depletion and oxidation of nucleobases respectively. Depletion of glutathione would induce cellular toxicity by compromising the antioxidant status of the cell whereas oxidation of nucleobases would cause DNA damage.

# ACKNOWLEDGMENTS

Fazlul Huq is grateful to the School of Biomedical Sciences, The University of Sydney for the time release from teaching.

### REFERENCES

- Cannavan, A., A.S. Haggan and D. Kennedy, 1998. Simultaneous determination of thiabendazole and its major metabolite, 5-hydroxythiabendazole, in bovine tissues using gradient liquid chromatography with thermospray and atmospheric pressure chemical ionisation mass spectrometry. J. Chromatogr., B, 718: 103-113.
- Chukwudebe, A.C., P.G. Wuslocki, D.R. Sanson, T.D.J. Halls and W.J.A. VandenHeuvel, 1994. In: Coulet, M., C. Eeckhoutte, G. Larrieu, J.-F. Sutra, L.A.P. Hoogenboom, M.B.M. Huveneers-Oorsprong, H.A. Kulper, J.V. Castell, M. Alvinerie and P. Galter, 1998. Comparative metabolism of thiabendazole in cultured hepatocytes from rats, rabbits, calves, pigs and sheep, including formation of protein-bound residues. J. Agric. Food Chem., 46: 742-748.
- Dalvie, D., E. Smith, A. Deese and S. Bowlin, 2006. In vitro metabolic activation of metabolism of thiabendazole in laying hen and lactating goats. J. Agric. Food Chem., 42: 2964-2969.
- Fujitani, T., M. Yoneyama, A. Ogata, T. Ueta, K. Mori and H. Ichikawa, 1991. New metabolites of thiabendazole by mouse embryo *in vivo* and *in vitro*. Food Chem. Toxicol., 29: 265-274.
- McKellar, A. and E.W. Scott, 1990. The benzimidazole anthelmintic agents-A review, Pharmacol. Therap., 13: 223-247.
- Mizutani, T., K. Ito, H. Nomura and K. Nakanishi, 1990. Nephrotoxicity of thiabendazole in mice depleted of glutathione by treatment with DL-buthionine sulphoximine. Food Chem. Toxicol., 28: 169-177.
- Mizutani, T., K. Yoshida and S. Kawazoe, 1993. Possible role of thioformamide as a proximate toxicant in the nephrotoxicity of thiabendazole and related thiazoles in glutathione-deleted mice: Structure-activity and metabolic studies. Chem. Res. Toxicol., 6: 174-179.
- Spartan '02, Wavefunction, Inc. Irvine, CA, USA., 2002.
- Tsuchiya, T., A. Tanaka, M. Fukukoa, M. Sato and T. Yamaha, 1987. Metabolism of thiabendazole and teratogenic potential of its metabolites in oregnant mice. Chem. Pharm. Bull., 35: 2985-2993.
- VandenHeuvel, W.J.A., P.G. Wislocki, D.R. Sanson, T.D.J. Halls and A.C. Chukwudebe, 1996. Metabolic fate of foliarly applied (<sup>14</sup>C) thiabendazole in three growing plants: Wheat, soybeans and sugar beets. J. Agric. Food Chain, 44: 2870-2877.